American Journal of Applied Sciences and Engineering | ***ISSN 2766-7596***
Published by ACADEMIC INK REVIEW | *https://airjournal.org/ajase*
12011 WestBrae Pkwy, Houston, TX 77031, United States
airjournals@gmail.com; enquiry@airjournal.org

Experimental Implementation of 2-Element Antenna Localization System for Small Cell Location Planning of Hetnets

Dorathy O. Abonyi
Department of Electrical and Electronic Engineering
Enugu State University of Science and Technology, Enugu, Nigeria

Publication Process	*Date*
Received	***July 29th, 2021***
Accepted	***August 20th, 2021***
Published	***August 31st, 2021***

ABSTRACT

In cellular heterogeneous networks, well-targeted small cells increase capacity, enhance coverage, offload traffic from the existing macro cell and ensure balanced load in the network. This paper experimentally demonstrates the use of a 2-element localization system for the purpose of small cell location planning. A centralized localization system that utilizes a differential 2-element antenna array to perform user localization and identify positions for small cell deployment is presented. The base station, which can also be the network gateway, is connected to two collinear antennas separated by λ/2. The relative phase of each antenna was varied using a phase shifter. The combined output of the two antennas was used to create sum and difference radiation patterns, and to steer the antenna radiation pattern to other angular positions. The system applies a simple RSSI based algorithm to calculate user AoA, range and user population per sector of the network to determine optimum positions for small cell deployment. Experiment with seventeen users in a LOS WiFi environment showed accurate angle of-arrival estimation and a range estimation with MAE of 2.19m relative to the BS. User clusters and positions for small cell deployment were correctly located.

Keywords: *Antenna Array; Antenna Radiation Patterns; RSSI; Azimuthal Angle; Distance Measurement; Heterogeneous Networks; 2-Element Antenna; Localization System; Small Cell Location Planning*

1. Introduction

In recent years heterogeneous networks (HetNet) and small cells have been utilized to help solve the problem of ever-increasing traffic demand caused by smart phones and other data hungry devices using the mobile cellular network facilities. In past years, homogeneous networks consisting of macro-cells were used to provide required capacity and coverage but recently due to the exponential growth in traffic demand and unavailability of BTS site especially in city centers HetNet became one of the feasible solutions that operators are using to achieve required capacity and coverage. HetNet is a network with different cell types and radio access technologies (RAT). In cellular network, small cells which include micro-, pico- and femtocells are deployed within the existing macrocell and integrated to work together forming a HetNet [1]. These small cells are low power, low complexity base transceiver stations (BTS) that are distinguishable by their power, coverage area, size, backhaul and propagation characteristics [2]. In cellular HetNet, appropriately deployed small cells improve capacity, enhance coverage and ensure good quality of service (QoS) to users [3], [4]. When small cells are deployed to alleviate coverage hot-zones, they offload high chunk of traffic from the big umbrella cell and ensure balanced load in the network [2]. Good small cell planning is required to ensure that small cells are deployed where they will be maximally used to achieve the objective of its deployment, minimize cost and avoid under-used network facility.

The technology of localization has been widely applied in different areas of wireless networks like navigation, environment sensing, home automation, human and animal condition monitoring, and recently in Internet of Things (IoT). The paper [5] proposed the use of a localization system as a strategy for prompt small cell deployment in HetNet with no details of the localization system implementation. This paper presents a hardware implementation of a 2-element localization system that will periodically scan a network coverage area to locate user clusters and identify locations for small cell deployment in a HetNet. If network operators are able to identify positions for small cell deployment at all times, they will be able to make good decisions on the appropriate locations as well as the type of small cells to be deployed to ensure balanced load and good QoS to users at all time.

Localization is the process of estimating the spatial coordinates of users scattered at unknown positions in space from at least one known location (base station). Two broad categories are rangefree and range-based localization. Range-free approach is based on proximity and determines user location using hop-counts or connectivity between network users. The hop-count values between base station (BS) and users are transformed to distance information based on the computed average size of a hop (hop-distance). With this approach, localization complexity increases as the network size increase. The range-based approach requires the knowledge of BS location from where user locations are calculated.

Currently localization can be achieved using time dependent methods such as time of arrival (TOA) [6], time difference of arrival (TDOA) [7] or global positioning systems (GPS). GPS based solutions provide high accuracy user positioning but suffer from concerns over user privacy [8] and indoor usage. Other time dependent approaches require regular synchronization which can be difficult to achieve in practice. Alternatively, received signal strength (RSS) based solutions can provide simple anonymous user data, requiring no extra hardware within the mobile handset but often rely on triangulation [9], [10] from adjacent BTS. In mobile cellular networks such solutions are therefore often only applicable near the cell edge as installing additional base station (BS) would increase the complexity and cost of a network deployment.

The localization system presented in this paper overcomes these limitations and can be easily incorporated in a mobile cellular network base transceiver station (BTS) to periodically monitor the cell coverage area and identify regions of high user concentrations for possible small cell deployment in heterogeneous networks. By deploying micro-, pico-, or femto-cells in areas of higher user concentration, high data rates and good quality of service in the network can be maintained. The network manager is provided with relative angle of arrival (AoA), distance and user cluster location to determine the relatively small cell deployment locations within the cell. The localization system divides the cell into a series of azimuthal and range sectors, and determines which sector the users are located in. Simulation of AoA and range estimation of users within a network coverage area was presented in [11]. Simulation results indicated system robustness to different levels of error in measured RSS. This paper presents an experimental implementation and testing of the system for the purpose of optimum small cell deployment position identification.

The rest of this paper is organized as follows; Section II presents the localization system model. Section III is the hardware implementation of the system. Section IV is the array summing implementation. Section V is the

localization algorithm while Section VI is experimental demonstration of system application and finally Section VII is the conclusion.

II. System Model

Consider a two element antenna array system separated by λ/2, where λ is wavelength of the radio signal. Elements are identical, omni-directional and vertically oriented as shown in Figure 1. Both elements are fed with the same power so that at same phase, signals arriving at both antennas from direction perpendicular to array axis add constructively forming a broadside main beam on azimuth in that direction as indicated in Figure 1. Because there are only two elements, the main beam is bi-directional with maxima at 90° and 270° and nulls at 0° and 180°. Considering a network coverage of only 180° and assuming [β1, β2] to be the phase states

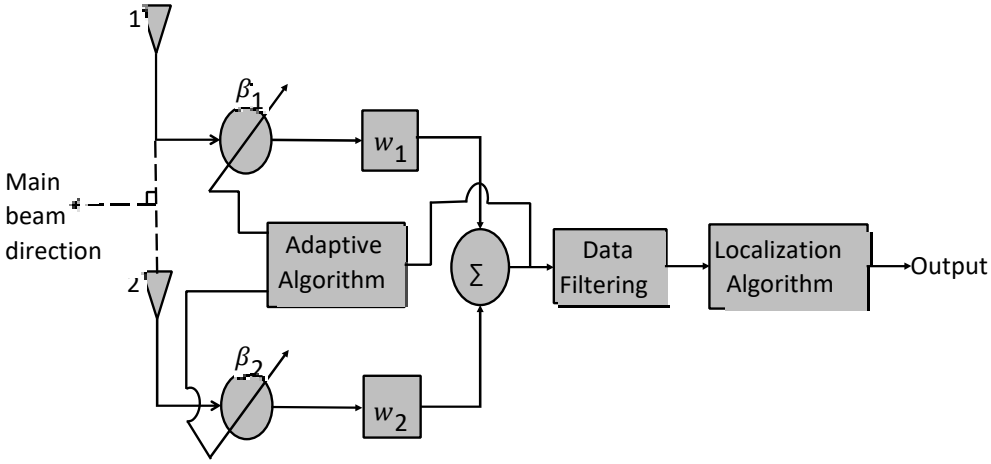

Fig. 1: Localization system block diagram used in this work

of Antennas [1, 2] respectively so that [0°, 0°] phase, places main beam at 90° to array axis. Assuming there is adaptive algorithm that updates the phase state of the individual elements using pre-calculated values, [120°, 0°], [0°, 120°], [180°, 0°] and [0°, 180°] to steering the main beam to other directions left and right of broadside. At each phase state, the weight of each elements which is given by $e^{jkzicos\theta+\beta i}$ for i^{th} antenna are summed as given by Equation 1 placing the main beam in the direction of interest and at the same time, nulls at the direction of no interest.

$$E = \sum_{i=1}^{n} e^{jkzicos\theta+\beta i}$$

where $z_i = (i-1)d = \frac{(n-1)d}{2}$ is the position of the ith antenna in the array, n is the number of antennas and d is the distance between the two elements.

At each beam position, the adaptive algorithm scans the network and measures RSSI from users found in the network. Data is filtered to removed interfering users and filtered data is used for AoA, range and user cluster localization. The system then outputs the optimum locations for small cell deployment with their relative coordinates.

III. System Implementation

The aim of this section is to achieve a hardware implementation of the designed localization system presented in the system block diagram of Figure 1. Implementation was carried out using 2.45GHz WiFi network because it uses industrial, scientific and medical (ISM) spectrum requiring no license like the cellular network would require. A schematic structure of the implementation is shown in Figure 2. The two antennas as designed are shown, separated by 61mm which is λ/2 for 2.45GHz frequency. Each antenna is connected through a phase shifter for phase weighting to a combiner for output summing. S1 and S2 are switches that are controlled to select a particular transmission line for phase shifter 1 (PS1) whereas S3 and S4 are the switches for phase shifter 2 (PS2). The adaptive algorithm block is achieved using ESP 8266 thing which digitally controls the switches via control points A and B as labeled and also

measures RSSI to be collected using a personal laptop for filtering, analysis and localization. The stages for implementation are presented in three main parts, the array system, phase weighting, and the adaptive algorithm implementations.

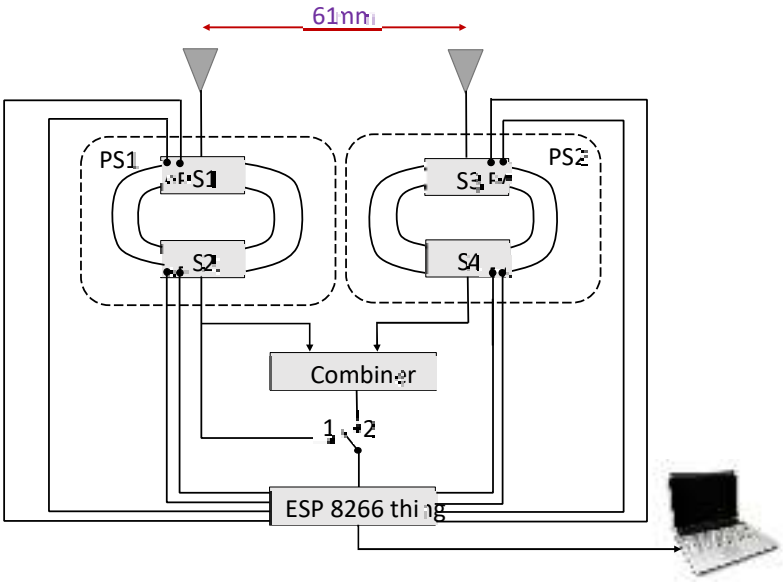

Fig. 2: Structural illustration of the observer system

A. Array System Implementation

RSSI is a composite output of environment and array gain, the higher the antenna gain, the stronger the received signal and the wider the coverage. Apart from considering an antenna that resonates at the desired frequency of operation, a high gain antenna was also desired. On the other hand, to achieve the desired beam on azimuth, the antennas need to be omni-directional and vertically polarized.

Array system was implemented using two pieces of antennas manufactured by RFTechnics Limited [12], with part number RFT-OMV-09-24. Each antenna is of 9dBi minimum gain, vertically polarized, collinear antenna having an omni-directional azimuth pattern operating in the 2.4GHz ISM band. The antenna is designed to be applied as access Point/Base Station for 802.11 b/g. Other features of the antenna that are of interest to this application include; suitability for both indoor and outdoor application, excellent performance across frequency band, no beam tilting is required which makes implementation easier and it has a nominal impedance of 50 ohms which gives assurance for impedance matching.

Input reflection coefficient (S_{11}) test of the two antennas were carried out to certify that there is good impedance matching that would guaranty transmission of most of the radio wave. Test was carried out using Agilent Technologies E5071B Vector Network Analyzer (VNA). Figure 3 shows the result obtained. From this result, S_{11} values at the antenna operating frequency band of 2.4 to 2.5GHZ are below −15dB which is less than the typical S_{11} value of −10dB. With the assumption that antennas are low loss, this means that negligible power will be reflected and so most of the power received by the array are delivered to the combiner.

1) **Antenna Array Testing:** Antenna array radiation was tested in the GBSAR anechoic chamber located at C22, Portobello building at The University of Sheffield, UK. This is a 6 × 4m partially anechoic chamber that was designed for synthetic aperture radar (SAR) measurements. The 2-element antenna array was placed on top of a turntable at a height of 1.1m at the center of the chamber (Figure 4 left). A 1 - 18GHz, transmitter horn antenna with 6.3dBi gain at 2.45GHz [13] was placed at one diagonal of the chamber at approximately the same height as the array (Figure 4 right), 3.4m from the array facing the anechoic part of the chamber. The horn antenna was connected to port 1 of the network analyzer and transmit power set to 0dBm (-30dB) from the computer control system. The array was vertically polarized and each of the antennas in the array system were connected to a combiner via a phase shifter with Antenna 1 connected to PS 1 and antenna 2 to PS2, making antenna 1 the reference antenna. Combined output of the two antennas was then connected to port 2 of the network analyzer.

The General Purpose Interface Bus (GPIB) port of the network analyzer was connected to a computer system from where the chamber was controlled and output data was collected and

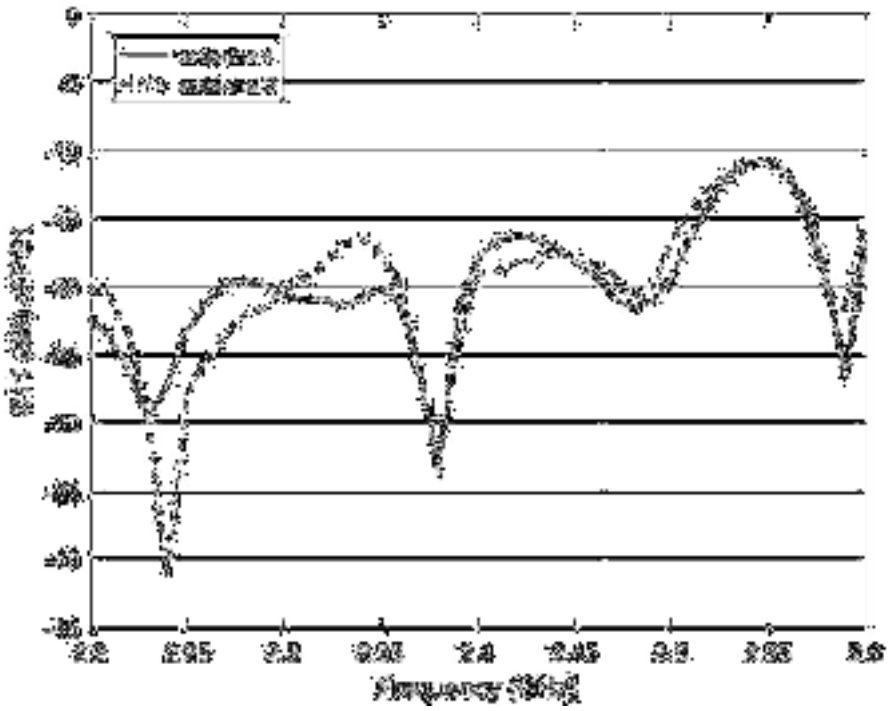

Fig. 3: Input reflection coefficient (S_{11}) test of the antennas used for the observer system implementation

Fig. 4: Array measurement in GBSAR anechoic chamber experimental setup inside the chamber saved. The phase shifters were controlled using ESP8266 thing module programmed in arduino IDE. Four measurements were performed for the required phase states of Table I.

TABLE I: System Control Truth Table

Phase state		Phase shifter1				Phase shifter2			
Ant 1	Ant 2	4 $S1_A$	5 $S1_B$	12 $S2_A$	13 $S2_B$	14(SCL) $S3_A$	GND $S3_B$	16 $S4_A$	Vcc $S4_B$

0	0	1	0	0	1	1	0	0	1
120	0	0	0	1	1	1	0	0	1
0	120	1	0	0	1	0	0	1	1
180	0	1	1	0	0	1	0	0	1

2) **Antenna Array Result and Analysis:** Measured radiation pattern at a frequency of 2.45GHz for the four phase states as well as free-space simulated pattern are shown in Figure 5. The simulation parameters include; transmitter power of −30dB ie 0dBm, transmitter gain of 6.3dB, receiver antenna gain is 9dB and distance of 3m. It can be seen that at same phase, main beam appears at angle 90° and it is moved to other directions at other phase selections as expected. This result has shown agreement with analytical beam-forming and beam-steering calculations.

Differences in measured RSS at peak positions between simulation and experiment for beams 1, 2, 3 and 4 are 0.83, 2.95, 2.95 and 5.31dB respectively. This result has shown a close relationship between experimental radiation pattern measured in anechoic chamber and simulation result.

B. Phase Shifter implementation

A simple switched line phase shifter was implemented using two HMC241ALP3E switches manufactured by Analog devices as switching elements and different calculated lengths of semirigid coaxial cables manufactured by Belden as RF transmission lines. The HMC241ALP3E is a general purpose non-reflective SP4T switch that operates at frequency band between 100 MHz to 4 GHz [14]. The switch operates at a single, positive supply voltage range of 3 to 5 Volts. A 2:4 line decoder is integrated on the switch providing logic control from two logic input lines to select one of the four radio frequency (RF) lines. The nominal velocity of RF propagation through the coaxial cable is 69.5% of the speed of light [15].

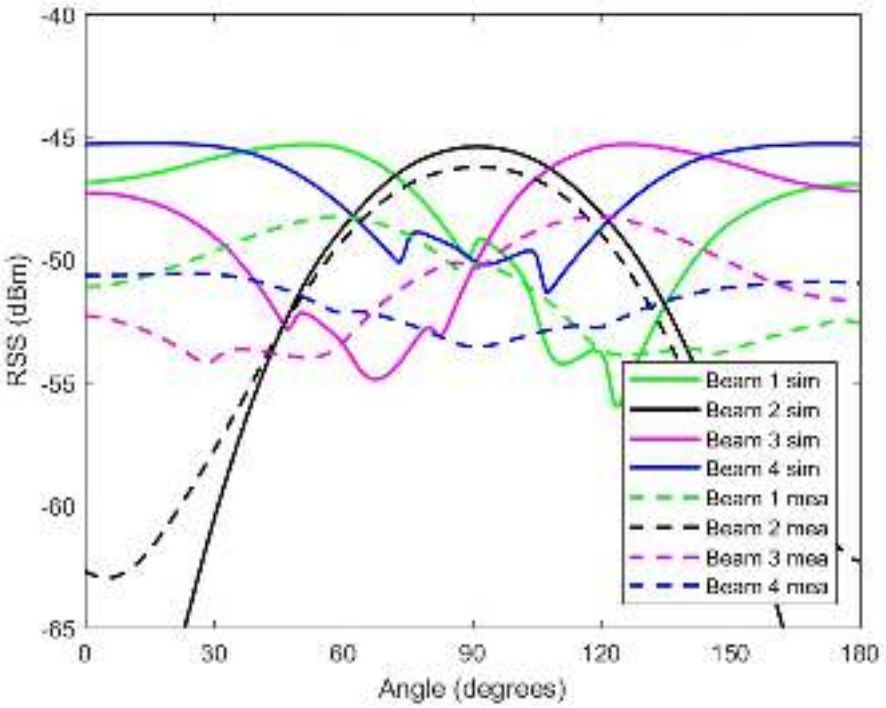

Fig. 5: Measured and simulated array radiation patterns at each beam steered positions

Considering the desired phases, antenna phase states which are 0, 120 and 180, a phase step of 60° was used to implement the phase shifters. Change in line length required to achieve the desired phase step is given by $\Delta L = (\Delta\phi \times \lambda n)/2\pi$, where ΔL is difference in line length between a delay line and the reference line. $\Delta\phi = 60°$ is required phase

step, π = 180° and λn = 85.1m/s is RF velocity as it propagates through this cable with nominal velocity of cable considered. ΔL was calculated to be 14.1mm.

Considering the minimum possible length that can be used to connect from the closest terminal of first evaluation board to the corresponding terminal of the second, the following cable lengths (86, 100, 114 and 128) mm were chosen for the design. SMA connectors were fitted at the ends of the cables and connected to the evaluation boards as implemented on the switched line phase shifter of Figure 6.

Considering the switch truth table on the data sheet of [14], a control truth table for our design was worked out as shown in Table II where $S1_A$, $S1_B$, $S2_A$ and $S2_B$ are control A of switch 1, control B of switch 1, control A of switch 2 and control B of switch 2 respectively.

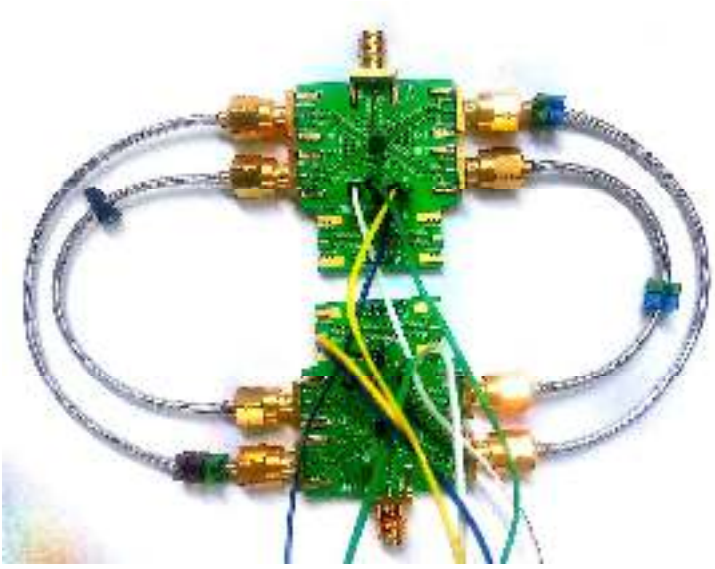

Fig. 6: Implemented switched line phase shifter using two HMC241ALP3E SP4T switches

TABLE II: Control Truth Table of SLPS design

A	B	Signal path state		$S1_A$	$S1_B$	$S2_A$	$S2_B$	Active lines
0	0	RF1		1	0	0	1	L1
1	0	RF2		0	1	1	0	L2
0	1	RF3		0	0	1	1	L3
1	1	RF4		1	1	0	0	L4

1) **Phase shifter Testing:** Flat phase shift over frequency can on its own be used to judge a phase shifter in a phased array application because it ensures that the pointing angle does not change even when there is a shift in frequency. The implemented phase shifters were tested using HEWLETT PACKARD 8720D 50MHz - 20GHz Vector Network Analyzer (VNA) at a center frequency of 2.45GHz and frequency span of 2GHz. The VNA carries out a relative phase measurement between the phase of the signal going into the phase shifter to the phase of its response signal which can be either reflected or transmitted. In all our test, we assumed that accurate calibration has been performed and so the difference in phase between the two signals (phase shift) is a result of the electrical characteristics of the phase shifter under test.

The two phase shifters were measured with primary focus on frequency range of 2.4GHZ to 2.5GHz with particular interest on the operating frequency of 2.45GHZ. Phase measurement of port 2 from port 1 (S21) was carried out. Phase shifter control for testing was achieved using ESP8266 module programmed in arduino following control states of Table II for each line test.

2) Phase Measurement: Phase shifter was calibrated on L1 of phase shifter 1 (PS1), all other delay lines (L2, L3 and L4) were tested. Still with calibration on PS1 L1, the second phase shifter 2 (PS2) was also tested to obtain the result of Figure 7. From this figure, the line phase at 2.45GH for PS1 (L1, L2, L3, L4) and PS2 (L1, L2, L3, L4) are (−0.5°, −53°, −103°, −164°) and (3°, −61°, −113°, −175°) respectively. In the same way, phase shifter 2, line 1 (PS2L1) was calibrated as the reference phase and all other lines of both phase shifters were tested. Result of Figure 8 gives a line phase of (−1°, −53°, −104°, −165°) and (0°, −64°, −116°, −178°) for PS1 and PS2 (L1, L2, L3 and L4) respectively. These results have shown that phase switching was achieved with this simple SLPS and so can be used to control the beam steering of the antenna array.

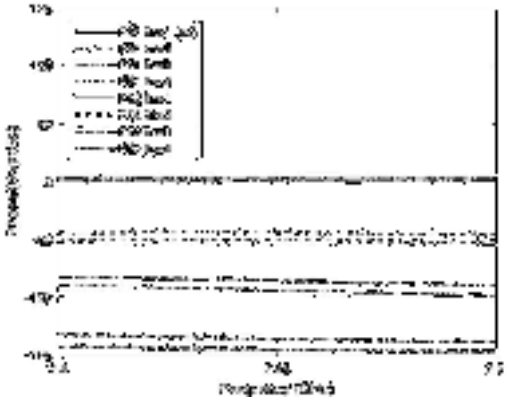

Fig. 7: Phase Switching between PS1 and PS2 with PS1 line 1 as reference

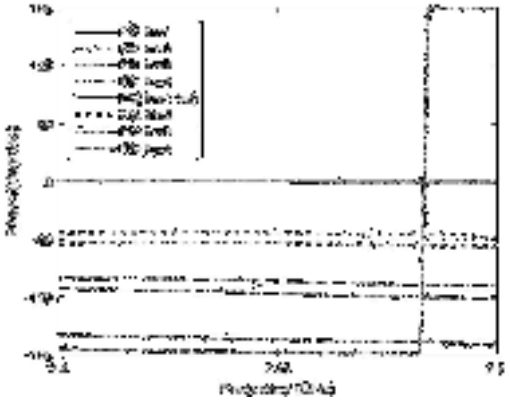

Fig. 8: Phase Switching between PS1 and PS2 with PS2 line 1 as reference

Our major interest with these phase shifters is achieving a steady phase over the 100MHz frequency band. These results have shown that using PS1 as the reference phase shifter, PS1 and PS2 lines L1, L2, L3 and L4 will have a phase deviation of 0.31°, 3.40°, 8.23°, 8.14° and 1.01°,

3.89°, 9.70°, 5.96° respectively giving a phase deviation mean of 5.08°. On the other hand, if PS2 is used as the reference phase shifter, PS1 and PS2 lines L1, L2, L3 and L4 will have a

phase deviation of 0.82°, 4.02°, 8.89°, 8.66°, 0.29°, 4.89°, 10.26° and 180° respectively giving a phase deviation mean of 27.23°. For a steady phase over frequency band, our desire is to achieve a difference of zero between the maximum and minimum phases measured in each transmission line across all frequencies within the frequency band. It is therefore clear that even though PS2 showed phase values closer to simulation, a steadier phase between both antennas over the required frequency band is better achieved by using PS1 as the reference phase shifter. This resolution is obvious in Figure 8 where PS2 is used as reference, at 2.48GHz frequency, the phase switched from −179 to +179. This is because the VNA does not display phase difference that is more than ±180°. This is so because measurement is made at discrete frequencies, and the data point at +180° and −180° may not be measured for the selected sweep. At the closest discrete value before the 180° value, the phase shift raps round through 180° phase difference. PS1 was therefore used as the reference phase shifter in the array testing because a more stable result is obtained with PS1 as reference phase shifter.

Return loss of the phase shifter was also tested to check how well the phase shifter will match to a 50 ohm impedance of the antenna. A typical S_{11} value is −10 or less [16] but result Figure 9 have shown S11 values below −11dB for a wider frequency band of 1.5 to 3.5GHz and below −15dB at required band of 2.4 to 2.5GHz for all transmission lines.

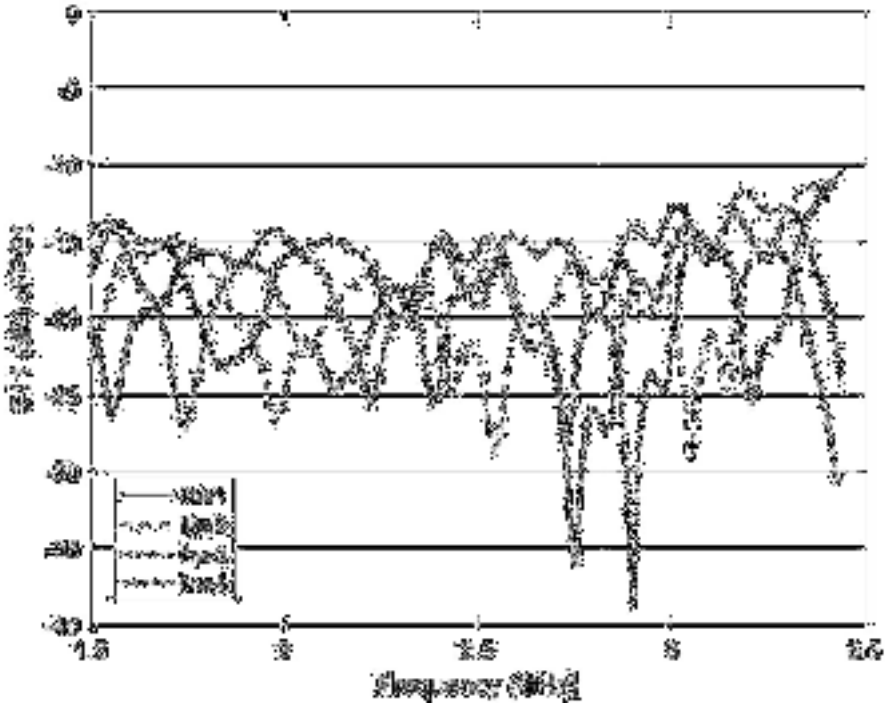

Fig. 9: Phase shift S11 measurement of PS1

IV. Summing Array Output Implementation

From the system block diagram of Figure 1, the signals from the two antennas needed to be summed and this was implemented using a two-way Fairview Microwave power divider/splitter (a.k.a combiner) with SMA connectors, part number MP8424-2. The power divider was rated for a minimum frequency of 2 GHz and a maximum frequency of 4 GHz according to the on-line datasheet [17] which makes it suitable for our application. It has a 50 Ohm impedance and a maximum input power of 30 Watts. To ensure good impedance matching and that no wave is reflected back, S_{11} measurement was carried out on the combiner using Agilent Technologies E5071B vector network analyzer (VNA). There are three ports in this combiner, the two input ports where antennas 1 and 2 are connected and the combiner output referred to as ports 1, 2 and 3 respectively. Figure 10 is the S_{11} measurement result of the combiner for frequency bands of 1.6 to 3.6GHz. From this figure, input reflection coefficients (Γ_{in}) for S_{31} and S_{32} is < −12

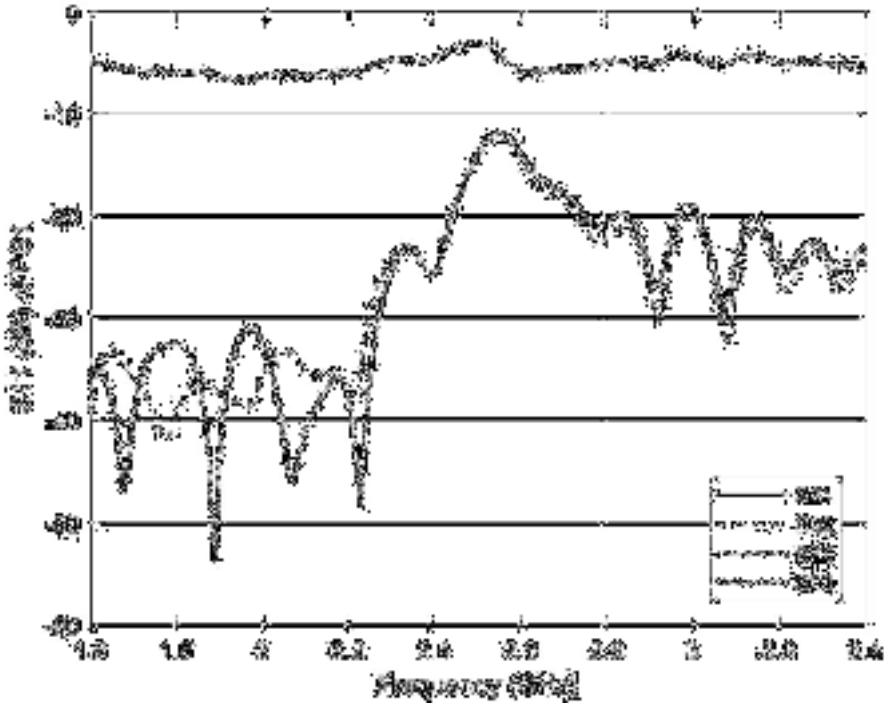

Fig. 10: Input reflection coefficient measurement (S11) of the 2 Way SMA power combiner to ensure proper impedance matching and good radio wave radiation

which means that most of the power coming in into ports 1 and 2 are delivered to port 3. (Γin) for S13 and S23 is approximately > −6 which is above the typical S11 value showing that most of the power delivered to port 3 is not reflected back to ports 1 or 2. Based on these results, it is believed most of the power from the antenna array will be received at the combiner output

for more reliable localization.

V. Localization Algorithm Implementation

Among some popular programmable boards like arduino uno, raspberry pie and an ESP8266thing [18], [19], an ESP8266thing was chosen for the algorithm implementation because of its cost effectiveness. Esp8266thing, popularly called the 'Thing' is cheap, has built-in WiFi and provision for an external antenna via the u.FL connector. It is development friendly due to its broken out pins and includes three opportunities for powering (LiPo, USB and battery). Easy to use for connecting things to the cloud. Most importantly, there is an ESP8266 board add-on which makes it possible for it to be programmed using the popular Arduino IDE. Unlike the arduinouno that has fourteen General Purpose Input/output (GPIO) pins, ESP8266 board has eleven I/O pins but that is sufficient for this project as only eight control pins are required.

SparkFuns ESP8266 new development board of Figure 11 was used for the hardware implementation of both the network users (Figure 12) as well as the system adaptive algorithm. Seventeen users were used in this project and each of them was programmed as WiFi access point (AP) with different SSID for identification. Users were programmed as APs so that they can host their own WiFi and BS can connect to them. The users were powered using three 1.5 volts batteries connected in series to achieve a 4.5 volt DC supply.

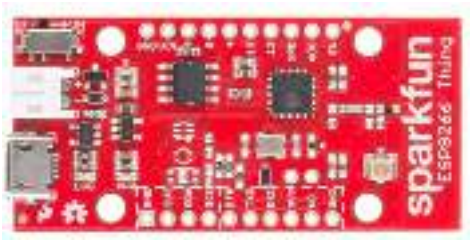

Fig. 11: ESP 8266 board

Fig. 12: Hardware implementation of network users

The localization system which is the BS was configured as station mode to be able to connect to the users and measure their RSSI. System was powered using a personal laptop. By interfacing a 3.3V Sparkfun FTDI basic with the Thing, C++ programs written in arduino IDE were uploaded to the Thing. The ESP8266WiFi.h library was included on the code to provide all required functionalities. A 0.1 second timer was set to provide some delays between processes. Pins 4, 5, 12, 13, 14, 16 as well as scanning time interval were declared. Pre-defined pin states of Table I were defined as an array. On the setup, serial communication was initialized to enable display of RSS via serial port. System was set to station mode and disconnected from all WiFi networks to allow connection to required networks. Additionally, all pins were initialized as an output pin. As a loop, the system connects to one antenna as an omni-directional antenna, scans the network to find users, if no user is found, the system re-scans the network until users are found. If users are found, the system declares the number of users found and captures measured RSS (dBm) of each user with their corresponding SSID. This process repeats for a total of ten scans. This is used as a reference to know users on the network that are to be located.

Next, the system starts the first iteration by activating the first row of the pin states to place the two elements at phases [0°,0°]. The system then carries out ten scans of the network and measure RSS in each case. The same process is carried out for all four iterations to obtain five data set of ten subsets each. Each subset is a set of all users found in the network with their measured RSS. The main sets are these subsets for ten scans obtained from reference, [0°,0°], [120°,0°], [0°,120°], [180°,0°] array phase scans. After a complete scan, the system delays for 20 seconds during which data is exported for analysis. Algorithm 1 is the system software implementation algorithm.

A picture of the implemented observer system is shown in Figure 13. The phase shifters are circled in red, combiners in yellow and Esp 8266 thing in purple. The brown lines represent the brown RG 142 RF cables used to connect the phase shifters to the antennas. Antennas 1 and 2 are shown as labeled. The red cable with USB end connects the output from ESP 8266 thing to a personal laptop as obviously shown.

Since our experiment was based on WiFi network, the system measures RSS from our users as well as all other WiFi networks in the same frequency band within the vicinity. Data filtering was therefore implemented to extract the deployed users which are users that belong to our network. RSSI of these users are then used for localization.

Algorithm 1 System Data Acquisition Algorithm

Step1: Starting up

1: start system and set timer

2: Set scanning interval

3: Define pin arrays for phase shifter control

4: Define pin array states

Step2: System and network Setup

5: Initialize serial communication

6: Set WiFi mode to station

7: Disconnect from any connected network 8: Initialize each pin as output

Step3: Find users in the network

9: Connect to one omni-directional antenna

10: Scan network, if no network is found, wait and re-scan until network is found

11: Count number of networks found and display

12: Measured RSS of all found networks and print with their individual SSID

13: Repeat scanning and RSS capture for ten scans

Step4: Collect data for localization

14: Switch system to antenna array

15: Activate first row of pin states array

16: Scan network

17: Measured RSS of all found networks and print with their individual SSID

18: Repeat scanning and RSS capture for ten scans

19: Update pin state and repeat scanning and RSS measurement for all pin array states.

20: Wait for a period of scanning interval and repeat process

VI. System Application for User Cluster and Small Cell Position Localization

Localization of users and finding position for small cell deployment was implemented using MATLAB script running on personal laptop. The implementation algorithm first calls up the filtration function to produce the measured RSS (filtered data) from the main beam positions as

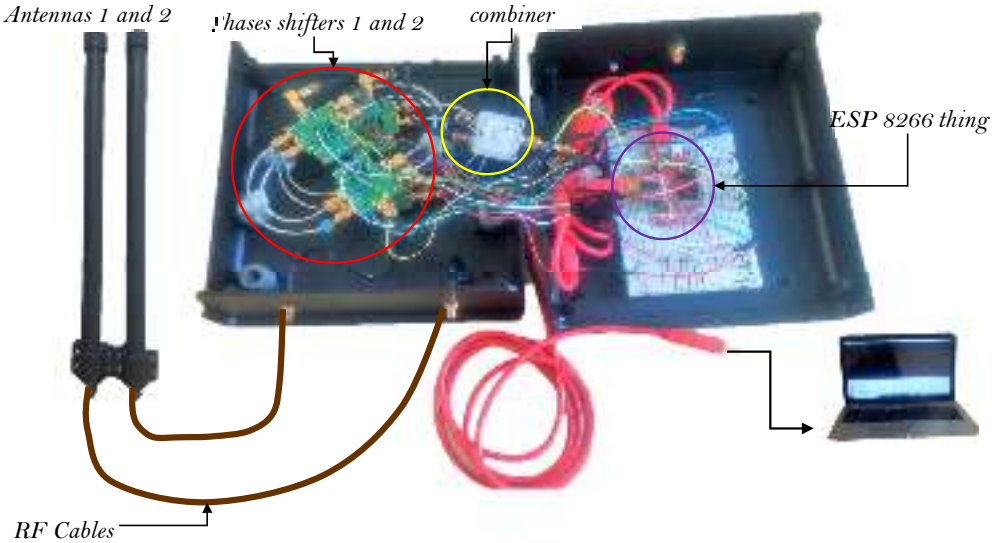

Fig. 13: Implemented hardware of the observer system showing both internal and external circuitries

given in Equation 2. These measured data are with some variation from expected value due to system and environment errors.

$$RSS_{\theta} = [RSS_{\theta 1}\, RSS_{\theta 2}\, RSS_{\theta 3}\, RSS_{\theta 4}]^{T}$$

The system first applies the AoA estimation model which is based on azimuth position that has measured maximum RSSI to estimate user sector angles. It then applies the Angle Adaptive Range Model (AARM) to estimate range of users based on their estimated AoA for four different line of sight environment scenarios differentiated by empirical path-loss models. The system calculates RSS-distance relationship using data at the beam peaks for the specified nominal range to develop range estimation model for each beam position. Depending on the estimated AoA of each user, the correct range estimation model is applied to estimate user range.

To improve the accuracy of estimated range, the system applies Beam Position Error Model (BPEM) which is error due to user azimuth position, Angular Deviation Error Model (ADEM) which is error due to users deviation from the azimuth center, Boundary User Error Model (BUEM) which is error peculier to boundary users. After all error models are applied, the output is a more accurate estimated range of the four environment models. The system then applies Environment Adaptive Range Model (EARM) to identify the closest environment that best describe the measured data. Estimated range of model returned by EARM is taken as the most accurate range estimate of users in the network. Using the accurate estimated range and the estimated AoA, users are classified into one of the azimuth-range sectors of the network coverage area. Due to few users used in this experiment, it is assumed that requirement for small cell deployment is minimum of two users. The system then counts the number of users

in each section and returns sections with users greater than two as positions requiring small cell deployment. Localization and small cell implementation are presented in Algorithm 2.

A. Outdoor Experimental Setup

Outdoor experiment was performed in the open field space at Ponderosa park in Sheffield as shown in the experimental setup picture of Figure 14. This is a rectangular space with dimension of approximately 100 × 50m featuring short grasses and with no obvious obstacle. A reference

Fig. 14: Outdoor experimental setup showing some of the distributed users on red and deployed observer system on yellow

position was taken at half the length of longer side (50m) and edge of the shorter side (0m). This position was considered as the reference, (0,0) coordinate position. Observer system was located at this position as circled with yellow marker and shown in Figure 14. This creates a rectangular coverage area with 50m space, left, right and in front of the observer system. The array elements were mounted on a tripod stand at a height of 0.9m. Phase shifters, combiners and other components were all coupled in a black plastic box of 198 × 188 × 70mm dimension and

Algorithm 2 System Localization Algorithm

Input:

Measured RSS RSSβ

Calculated range

BPEM

ADEM

BUEM

Output:

Estimated user AoA

Estimated user range

Small cell deployment positions

1: Estimate AoA of users using AoA Estimation model

2: for *Rm* = 1 to number of environments do . range models are FSPL, HATA, ITU, WINNER-11

3: for *users* = 1 to number of users do

4. Estimate range of users using angle adaptive range model (AARM), R_{AARM}

5. Apply BPEM to estimated range, R_{BPEM}

6. Apply ADEM to R_{BPEM} to obtain R_{ADEM}

7. Apply BUEM to R_{ADEM} to obtain R_{BUEM}

8. $UR = R_{BUEM}$. estimated range of users is the range after BUEM for all models

9. Apply EARM to determine model with best range model

10. $UR = R(Rm)_{EARM}$. accurate estimated range of users is the range estimated by the predicted environment model
11. Allocate users into created azimuth and range positions based on estimated AoA and Range

12. Count number of users in each position section

13. If section user count ≥ small cell requirement, circle position for small cell deployment

14. Print coordinates of small cell deployment positions

---

was mounted by the side of the tripod stand. System was powered using a fully charged personal laptop which also do the data capturing using RealTerm serial monitor as well as processing and localization in Matlab. Seventeen users were used in this experiment and were placed within the rectangular coverage area some of which were captured by the camera and circles in red markers as shown in Figure 14.

A model of the deployment and actual users locations are shown in Figure 15. RSS was measured as expected and mean measured RSS result shown in Figure 16.

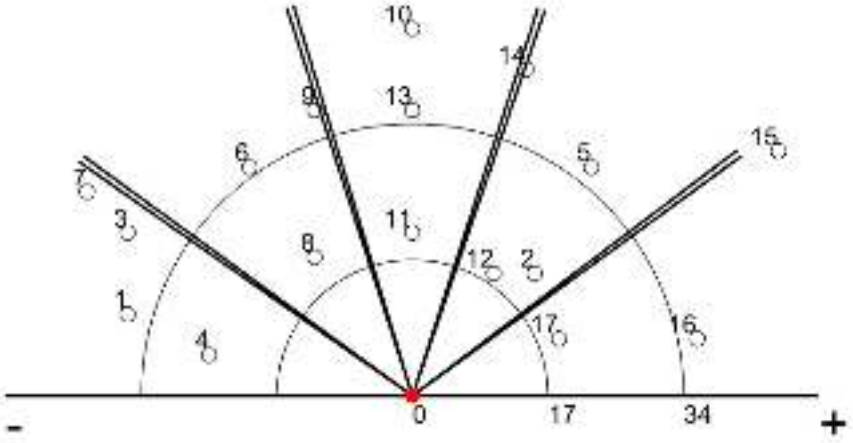

Fig. 15: Actual user position before localization

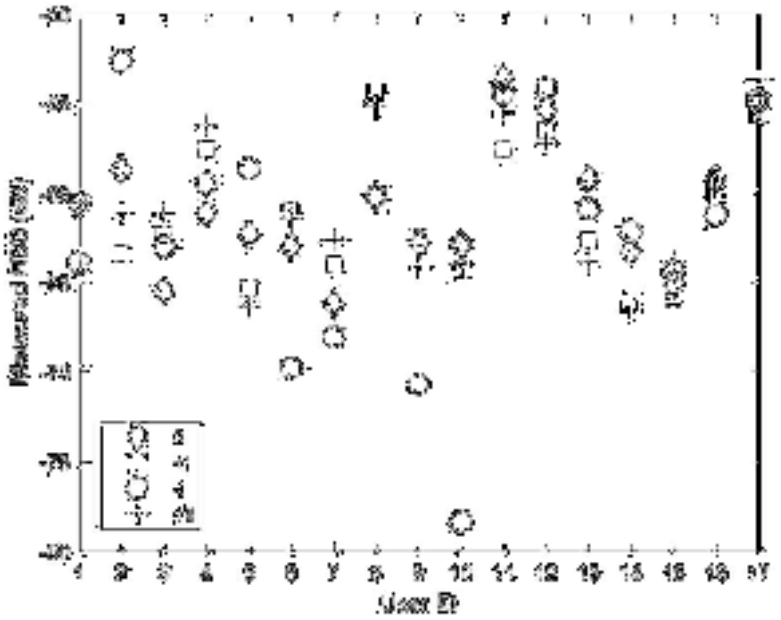

Fig. 16: User deployment for final experiment showing measured RSS from user devices at all azimuth positions

From this result, it can be seen that all seventeen users were identified and it is obvious that for each user, only one azimuth position has recorded highest RSS compare to other azimuth positions. This shows that users can be classified into azimuth positions using highest measured RSS. Using mean measured RSS for each user at all azimuth positions, the system applies the AoA estimation model to estimate user azimuth positions. Figures 17 is the estimated AoA of users using experimental data with the highest measured RSS of each user printed beside it. The system applies all four range estimation models using the measured RSS as input data in each case to estimate user range with all error model applied. All estimated range were then used to predict environment of measurement. Result of Figure 18 shows the experimental estimated range with actual and simulated range for each user.

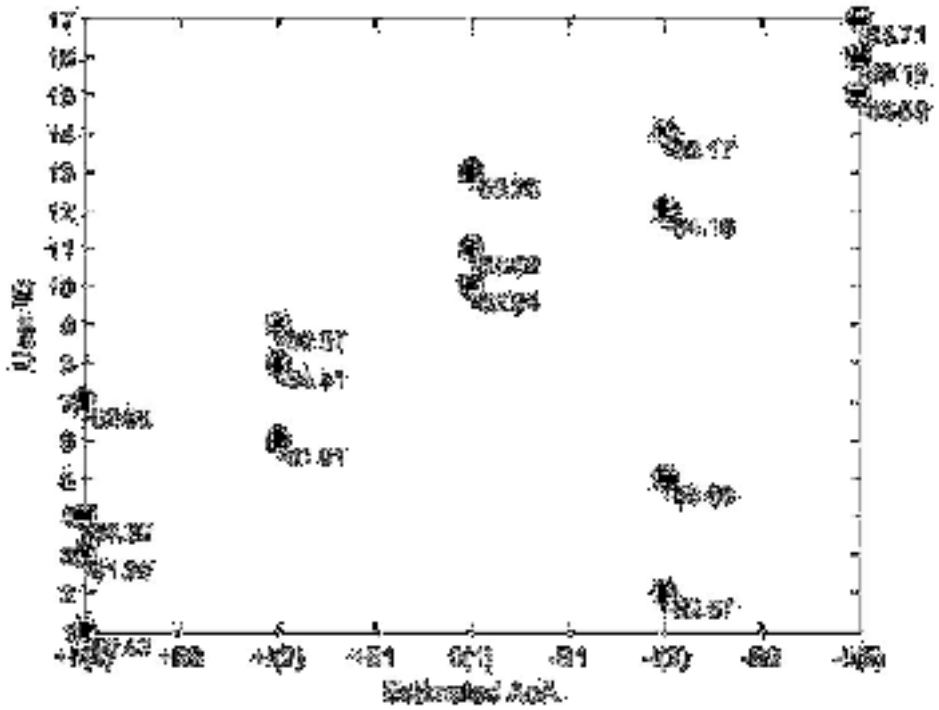

Fig. 17: Experimental AoA estimation Results

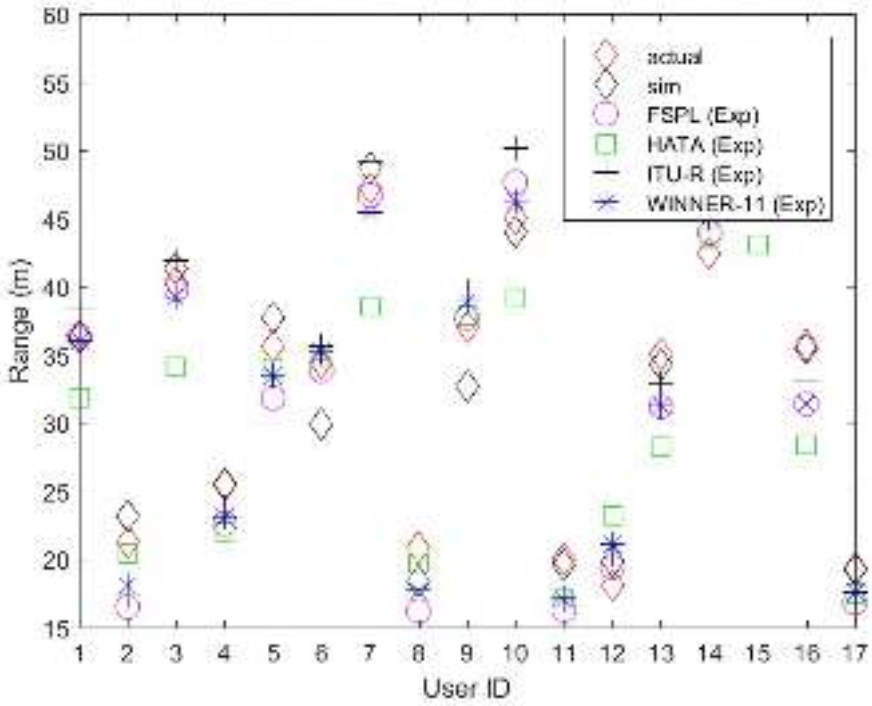

Fig. 18: Estimated range of users using all four range models with experimental measured RSS as input

Comparing the estimated azimuth AoA with actual user azimuth positions of Figure 15, result has shown 100% accuracy in range estimation for the distributed users. Range estimation result of Figure 18 has shown a close relationship between actual, simulated and experimental results with mean absolute error in range estimation of 2.13m between experimental and actual range.

The system algorithm is then applied to estimate user clusters and small cell deployment positions. Network area was shared into three equal range locations because of small experimental nominal range. A small cell deployment threshold of 2 is also assumed due to few numbers of users used in this experiment. Figures 19 and 20 show the located user clusters with positions for small cell deployment indicated by circling and the coordinates of the deployment positions relative to the BS respectively.

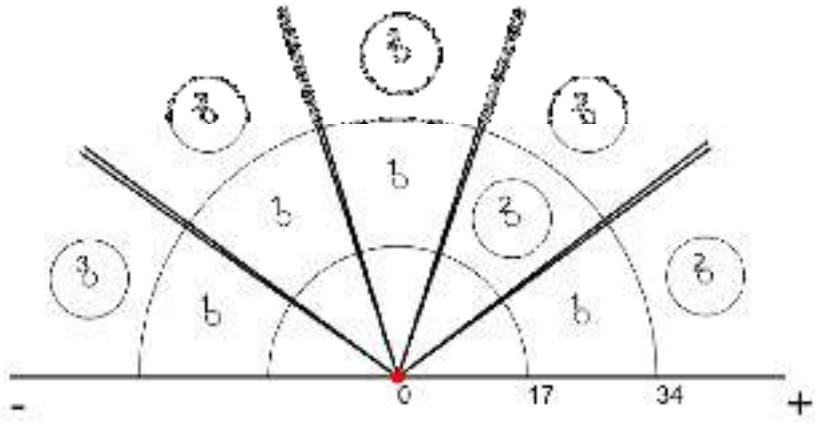

Fig. 19: Experimental small cell deployment strategy showing user cluster localization

x_cordinate_Exp	y_cordinate_Exp	Population_Exp
-40	13	3
-24	34	2
0	42	2
16	29	2
24	34	2
40	13	2

Fig. 20: Experimental small cell deployment strategy showing small cell deployment position coordinates relative to BS

Matching the user cluster localization result with the actual user location of Figure 15, it is certain that users have been correctly located into their relevant clusters. The system has also been able to correctly identify positions for small cell deployment. This experiment has shown 100% accuracy for the deployed users. It should be noted that this may not be the case for a larger coverage area and for smaller cluster localization area but it shows that high accuracy is most likely to be achieved.

VII. Conclusions

A hardware implementation of 2-element antenna localization system that would help wireless network operators identify locations for small cell deployment has been presented. The system calculates user AoA and range to determine user clusters and estimate optimum positions for small cell deployment based on number of users per

cluster. Experimental result of seventeen users have shown accurate AoA and range estimation with a MAE of 2.19m. System was able

to correctly identify user cluster and positions for small cell deployment. Deploying small cells within high user concentration areas will offload traffic from the macrocell, ensure balanced load

and good QoS to customers. In general, system has shown good performance for the purpose of identifying optimum location for small cell deployment in a HetNet.

REFERENCES

Salim S.; Oey, C.; and Moh, S. (2012). Are Heterogeneous Cellular Networks Superior to Homogeneous Ones? *Lecture Notes in Computer Science,* 75(13), 61–68. [Online]. Available: https://hal.inria.fr/hal-01551342

Ghosh A., Mangalvedhe, N.; Ratasuk, R.; Mondal, B.; Cudak, Visotsky, M. Thomas, E. T.; Andrews, J.; Xia, P; Jo, H.; Dhillon, H.; and Novlan, T. Heterogeneous cellular networks: From theory to practice, *IEEE Communications Magazine,* 50(6), 54–64. [Online]. Available: http://ieeexplore.ieee.org/document/6211486/

Chu, N. E, X. and Zhang, J. (2015). Mobile Small-Cell Deployment Strategy for Hot Spot in Existing Heterogeneous Networks, IEEE Globecom Workshops (GC Wkshps). *IEEE, 1–6.* [Online]. Available: http://ieeexplore.ieee. org/document/7414060/

Khandekar, A.; Bhushan, N.; Tingfang, J. and Vanghi, V. (2010). LTE-Advanced: Heterogeneous Networks. *European Wireless Conference*, 978–982. [Online]. Available: https://pdfs.semanticscholar.org/dedb/ af87573ee403c1173f3c69908ce888569dc9.pdf

Abonyi, D. (2019). A Novel Strategy for Prompt Small Cell Deployment in Heterogeneous Networks. *Advances in Science, Technology and Engineering Systems Journal (ASTES),* 265–270. [Online]. Available: https://https: //www.astesj.com/publications/ASTESJ 040433/

Vaghefi, R. M. and Buehrer, R. M. (2013). Asynchronous time-of-arrival-based source localization, *IEEE International Conference on Acoustics, Speech and Signal Processing,* 4086–4090. [Online]. Available: http: //ieeexplore.ieee.org/document/6638427/

Ghelichi, A.; Yelamarthi, K. and Abdelgawad, A. (2013). Target localization in Wireless Sensor Network based on Time Difference of Arrival, in 2013 IEEE 56th International Midwest Symposium on Circuits and Systems (MWSCAS). IEEE, pp. 940–943. [Online]. Available: http://ieeexplore.ieee.org/document/6674805/

Rao, S. P.; Oliver, I.; Holtmanns, S.; and Aura, T. (2016). We know where you are, in 2016 8th International Conference on Cyber Conflict (CyCon). *IEEE,* 277–293. [Online]. Available: http://ieeexplore.ieee.org/document/7529440/

Thrivikrama, V.; Ashok, G.; and Srinivas, A. (2011). A novel two-stage self-correcting GPS-free localization algorithm for GSM mobiles, Fifth IEEE International Conference on Advanced Telecommunication Systems and Networks (ANTS). IEEE, pp. 1–6. [Online]. Available: http://ieeexplore.ieee.org/document/6163634/

Kristalina, P.; Pratiarso, A.; Badriyah, T.; and Putro, Erik Dwi (2016). A wireless sensor networks localization using geometric triangulation scheme for object tracking in urban search and rescue application, in 2016 2nd International Conference on Science in Information Technology (ICSITech). IEEE, pp. 254–259. [Online]. Available: http://ieeexplore.ieee. org/document/7852643/

Abonyi, D. and Rigelsford, J. (2018). A System for Optimizing Small-Cell Deployment in 2-Tier HetNets, in 2018 IEEE 23rd International Workshop on Computer Aided Modeling and Design of Communication Links and Networks (CAMAD). IEEE, pp. 1–6. [Online]. Available: https://ieeexplore.ieee.org/document/8514981/

RFTechnics, 9 dB Omnidirectional Antenna. [Online]. Available: http://www.rftechnics.com/data/RFT {\} OMV {\} 09{\ }24{\} Antenna.pdf

C. Qwh-sl, 0. 5 - 2 GHz Linearly Polarised Wideband Ridged Horn Antenna fitted with an N type Connector, Steatite, Tech. Rep.

A. Devices, hmc241 (v00.0513). [Online]. Available: www.hittite.comhttp://www.analog.com/media/en/ technical-documentation/data-sheets/hmc241.pdf

Insulation Insulation Material: Insulation Trade Name Insulation Material Dia. (in.) Mechanical Characteristics (Overall) Applicable Specifications and Agency Compliance (Overall). [Online]. Available: http://www.farnell.com/datasheets/2335138.pdf?

{\}ga=2.152187581.561354287.1510939522108064745 9.1493736609{\&} {\} gac=1.245690032. 1510569556.EAIaIQobChMI{\ }4-Lha671wIVqRXTCh0K-QuQEAQYAyABEgKkJ {\} D {\} BwE

K.-J. Koh and G. M. Rebeiz, (2007). 0.13-µm CMOS Phase Shifters for X-, Ku-, and K-Band Phased Arrays, *IEEE Journal of Solid-State Circuits,* 42(11), pp. 2535–2546, [Online]. Available: http://ieeexplore.ieee.org/document/ 4362098/

2 Way Power Divider SMA Connectors From 2 GHz to 4 GHz Rated at 30 Watts. [Online]. Available: https://www. fairviewmicrowave.com/2-way-power-divider-sma-4-ghz-30-watts-mp8424-2-p.aspx

Marot J. and Bourennane, S. (2017). Raspberry Pi for image processing education, 25th European Signal Processing

Conference (EUSIPCO). IEEE, pp. 2364–2366. [Online]. Available: http://ieeexplore.ieee.org/document/8081633/

Ok, F.; Can, M.; Ucgun, H.; and Yuzgec, U. (2017). Smart mirror applications with raspberry Pi. *International Conference on Computer Science and Engineering (UBMK)*, 94–98. [Online]. Available: http://ieeexplore.ieee. org/document/8093566/

Authorship

Dr. Dorathy Obianuju Abonyi has a PhD and a Master of Science (MSc) degrees in Electronic and Electrical Engineering from The University of Sheffield, United Kingdom as well as a Master of Engineering (M.Eng) and Bachelor of Engineering (B.Eng) degrees of the Enugu State University of Science and Technology (ESUT), Enugu, Nigeria. She is currently a Lecturer at the Department of Electrical and Electronic Engineering, ESUT. Her area of interest includes wireless communications, antenna, Radio wave propagation and Internet of Things (IoT). Dorathy is happily married and blessed with lovely children.